Excitation of rotational modes in two-dimensional systems of driven Brownian particles

Udo Erdmann* and Werner Ebeling
Institute of Physics, Humboldt University Invalidenstraße 110, 10115 Berlin, Germany

Vadim S. Anishchenko
Department of Physics, Saratov State University, 410026 Saratov, Russia

(Received 24 July 2001; revised manuscript received 7 January 2002; published 18 June 2002)

Models of active Brownian motion in two-dimensional (2D) systems developed earlier are investigated with respect to the influence of linear attracting forces and external noise. Our consideration is restricted to the case that the driving is rather weak and that the forces show only weak deviations from radial symmetry. In this case an analytical study of the bifurcations of the system is possible. We show that in the presence of external linear forces with only small deviations from radial symmetry, the system develops rotational excitations with left-right symmetry, corresponding to limit cycles in the 4D phase space, the corresponding distribution has the form of a hoop or a tire in the 4D space. In the last part we apply the theory to swarms of Brownian particles that are held together by weak and attracting forces, which lead to cluster formation. Since near the center the potential is at least approximately parabolic and near to the radial symmetry, the swarm develops rotational modes of motion with left-right symmetry.

DOI: 10.1103/PhysRevE.65.061106 PACS number(s): 05.40.Jc, 05.45.Xt, 47.32.Cc, 87.18.Ed

I. INTRODUCTION

Recently several papers describing coherent motions of swarms were published [1–14]. It was shown there that relatively simple physical models can be used to describe complex behavior of moving clusters in physics [3,15], biology [6,8,9,14,16] and social systems [11,12,17]. In many of these published works, spontaneous motions of clusters were shown to arise from a self-propelling feature of individual particles [1,5,6,8–10,13].

In [1,5,10,11,16] the influence of noise on the coherent behavior of the swarms was studied. In most of the cases a phase transition in the type of coherent motion was predicted, with increasing noise. Rotational modes, or vortex states, were observed, for example, in Ref. [5]. Vortex states, objects of high current interest, can be used for the description of flocks of birds [2,7], systems of dusty plasmas [3], and bacteria in a Petri dish [4,6,9,13].

In earlier papers [18–20] we introduced a generalized idea of stochastically moving species, active Brownian particles. We want to recall this approach that will be used later on. Active Brownian particles are Brownian particles with the ability to take up energy from the environment and use it for the acceleration of motion. Simple models composed of active Brownian particles were studied in many earlier works [21–24]. As already mentioned flocking behavior was described by interacting mechanisms so far [25]. The concept of self-propelled particles [1] leads to flocking behavior because of locally interacting particles that differ from previous models due to an intrinsic driving force. In this paper we extend previous studies to include the interplay of self-propelling features and direct interaction forces simultaneously that lead to the rotating clusters or to oscillating clusters in one dimension (1D) [10]. This paper unites the active motion concept, for example self-propelling particles, with direct particle-particle interaction. This results in a wider variety of possible models especially for biological systems. While previous studies [1,5,25] were able to describe simple collective motions, they were unable to accommodate properties of individual particles, for example, specific attractive interactions that would lead to swarming.

The question that will be addressed here is; why can clusters of interacting particles collect as a swarm and then rotate as, for example, exhibited by flocks of birds, and what could be a plausible reason for these motions. Another problem we would like to address is; what is the consequence of broken radial symmetry of the swarm, can spontaneous rotations be stopped by certain amount of asymmetry?

In contrast to previous studies [1,4,5,13] the self-propelling feature is modeled by active Brownian particles with negative friction [18–20,26] that are able to convert stored internal energy into motion. As we show below, this self-propelling feature combined with the attractive particle-particle interaction is a sufficient reason accounting for the formation of swarms and this subsequent vortexlike motion.

We will start our investigations by adding to the dynamics of simple physical Brownian particles different mechanisms such as pumping with free energy, which may be realized in several steps as by energy take up, storage and conversion of energy, and energy consuming motion. In this way, the particle motions become more complex resulting in dynamical features that may resemble active biological motions. Hence, the basic idea can be formulated as follows: how much physics is needed to achieve a degree of complexity that gives us the impression of motional phenomena found in biological systems? We will come back to this question in the last part.

In this paper, we will study only the motion in external fields on a plane ($d=2$). In particular we are interested in rotational motions that are excited by the coupling of nonlinear velocity-dependent (negative) friction terms and interaction forces that can be described by a mean field.

*Electronic address: udo.erdmann@physik.hu-berlin.de

In Sec. II, we revisit the idea of pumping by negative friction and outline the basic dynamics of our model including Langevin and Fokker-Planck equations.

In Sec. III we outline our previous studies of rotationally symmetric external potentials.

In Sec. IV we consider the case of active Brownian motion in external potentials without rotational symmetry, in particular, in asymmetric parabolic potentials.

In Sec. V we discuss applications of the theory to rotational excitations of pairs, clusters and swarms.

II. EQUATIONS OF MOTION FOR ACTIVE BROWNIAN DYNAMICS

The motion of Brownian particles with velocity-dependent friction can be described by the Langevin equation,

$$\dot{\boldsymbol{r}}=\boldsymbol{v}; \quad m\dot{\boldsymbol{v}}=-\gamma(\boldsymbol{v})\boldsymbol{v}-\boldsymbol{\nabla}U(\boldsymbol{r})+\boldsymbol{\xi}(t), \tag{1}$$

where $\gamma(\boldsymbol{v})$ is the effective friction function of the particle with mass m at position $\boldsymbol{r}$, moving with velocity $\boldsymbol{v}$. $U(\boldsymbol{r})$ can be either an external potential or the result of a mean field. In the following we will choose units in which $m\equiv 1$. $\boldsymbol{\xi}(t)$ is a stochastic force with strength D and a δ-correlated time dependence,

$$\langle \boldsymbol{\xi}(t)\rangle=0; \quad \langle \boldsymbol{\xi}(t)\boldsymbol{\xi}(t')\rangle=2D\,\delta(t-t'). \tag{2}$$

In the case of systems in thermal equilibrium, with $\gamma(\boldsymbol{v})=\gamma_0=\text{const}$, we may assume that the loss of energy resulting from friction, and the gain of energy resulting from the stochastic force, are compensated in the average. In this case the fluctuation-dissipation theorem (Einstein relation) is,

$$D=k_B T\gamma_0, \tag{3}$$

where T is the temperature, k_B is the Boltzmann constant, and D is a scaled expression for the strength of the stochastic force in the velocity space.

In this paper we are mainly interested in the influence of forces and interactions where velocity-dependant pumping plays an important role as found, for example, in certain models of the theory of sound developed by Rayleigh [27]. In the simplest case we may assume the following friction function for an individual Brownian particle:

$$\gamma(\boldsymbol{v})=-\alpha+\beta\boldsymbol{v}^2=\alpha\left(\frac{\boldsymbol{v}^2}{\boldsymbol{v}_0^2}-1\right). \tag{4}$$

This Rayleigh-type model is a standard model studied in many papers on Brownian dynamics [21]. We note that $\boldsymbol{v}_0^2=\alpha/\beta$ defines a special value of the velocities such that the effective friction is zero. A somewhat different model for active friction with a zero point $\boldsymbol{v}_0$ was introduced and treated by the authors of Refs. [18,19]. There the friction function is based on the a model of Brownian motion with energy depot. The authors of Refs. [18–20] assume that the Brownian particle itself is capable of taking up external energy and storing some of this in an internal energy depot, $e(t)$. This depot model leads to the friction function

$$\gamma(\boldsymbol{v})=\gamma_0-\frac{d_0 q_0}{c+d_0\boldsymbol{v}^2}, \tag{5}$$

where q_0 the rate of the energy uptake, c the strength of internal dissipation, and d_0 the conversion rate of internal energy into energy of motion.

Due to the pumping slow particles are accelerated and fast particles are damped. For certain conditions, the active friction functions have a zero corresponding to the stationary velocity $\boldsymbol{v}_0$, where the effective friction disappears. The deterministic trajectory of the system is in both cases attracted by a cylinder in the 4D phase space [20,28] given by

$$v_1^2+v_2^2=\boldsymbol{v}_0^2, \tag{6}$$

where $\boldsymbol{v}_0$ is the value of the stationary velocity which for the Rayleigh-model, is given by $\boldsymbol{v}_0^2=\alpha/\beta$ and for the depot model by $\boldsymbol{v}_0^2=q_0/\gamma_0-c/d_0$. The parameter $\mu=\alpha/\beta$ in the Rayleigh model and $\mu=q_0/\gamma_0-c/d_0$ for the depot model plays the role of a bifurcation parameter. Both the Rayleigh-model and the depot model show a bifurcation if μ becomes greater than zero, i.e., $\boldsymbol{v}_0$ becomes real. If the bifurcation parameter is greater then zero in both models the system is in the pumping regime. For $\mu<0$ the particles behave similar to the classical friction case.

We will restrict here our study to the case of rather weak driving forces. Near to the bifurcation point both models may be unified. Therefore we use the Rayleigh model for all further investigations.

The stationary solutions of the Fokker-Planck equation for the probability distribution $P(\boldsymbol{r},\boldsymbol{v},t)$

$$\frac{\partial P}{\partial t}=-\boldsymbol{v}\cdot\frac{\partial P}{\partial \boldsymbol{r}}-\nabla U(\boldsymbol{r})\cdot\frac{\partial P}{\partial \boldsymbol{v}}+\frac{\partial}{\partial \boldsymbol{v}}\cdot\left\{\gamma(\boldsymbol{v})\boldsymbol{v}P+D\frac{\partial P}{\partial \boldsymbol{v}}\right\} \tag{7}$$

reads for the Rayleigh model [20]

$$P_0(\boldsymbol{v})=C\exp\left[\frac{\beta\boldsymbol{v}^2}{2D}\left(\mu-\frac{1}{2}\boldsymbol{v}^2\right)\right]. \tag{8}$$

The shape of this distribution Eq. (8) can be seen in Fig. 1. A bifurcation to limit cycle at $\mu=0$ can be seen for the noisy system. It is obvious that the system above the bifurcation point is far from equilibrium and shows a permanent motion of the particles. Noise mediated Hopf bifurcations were earlier studied in Refs. [29,30].

III. ACTIVE MOTION IN EXTERNAL POTENTIALS WITH ROTATIONAL SYMMETRY

For further investigations, let us summarize results found in earlier works [18–20]. We specify the potential $U(\boldsymbol{r})$ as a symmetric parabolic potential:

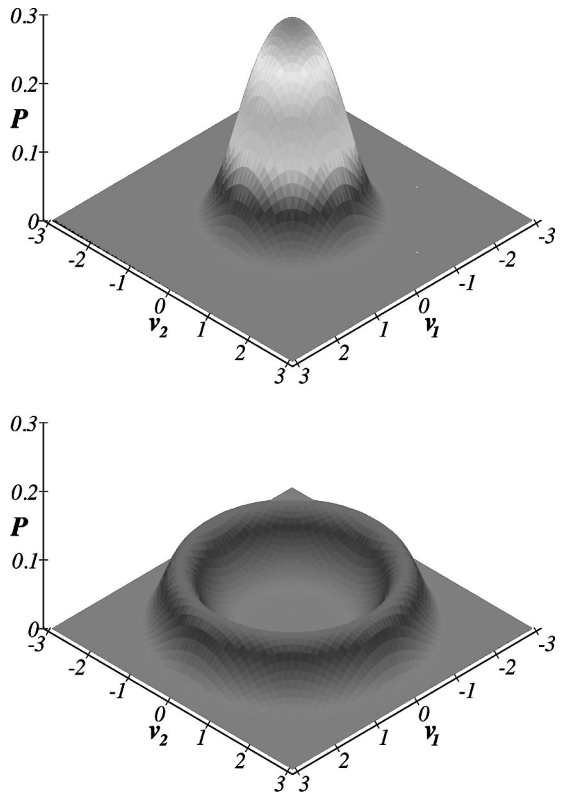

FIG. 1. Normalized stationary distribution $P_0(v_1,v_2)$ of the noisy fixed point and limit cycle in the velocity space for increasing values of $\mu=-1.0$ (upper), $\mu=4.0$ (lower), $\beta=1.0$.

$$U(x_1,x_2)=\frac{1}{2}a(x_1^2+x_2^2). \tag{9}$$

First, we restrict the discussion to a deterministic motion, which then is described by the differential equations:

$$\ddot{x}_1=-\gamma(v_1,v_2)v_1-ax_1, \tag{10a}$$

$$\ddot{x}_2=-\gamma(v_1,v_2)v_2-ax_2. \tag{10b}$$

For the one-dimensional Rayleigh-model this system possesses a limit cycle corresponding to sustained oscillations with the energy $E_0=\alpha/\beta$.

For the 2D case we have shown in Ref. [20] that a limit cycle in the 4D phase space is developed. The projection of this periodic motion on the $\{v_1,v_2\}$ plane and on the $\{x_1,x_2\}$ plane are circles

$$\begin{aligned} v_1^2+v_2^2&=v_0^2=\text{const},\\ x_1^2+x_2^2&=r_0^2=\text{const}. \end{aligned} \tag{11}$$

The limit cycle energy is

$$E_0=\frac{v_0^2}{2}+\frac{a}{2}r_0^2. \tag{12}$$

It has been shown in Ref. [18], that any initial value of the energy converges (at least in the limit of strong pumping) to

$$H\rightarrow E_0=mv_0^2. \tag{13}$$

This corresponds to an equal distribution between kinetic and potential energy, i.e., both parts contribute the same amount to the total energy. The motion on the limit cycle in the 4D space may be represented by the four equations

$$\begin{aligned} x_1&=r_0\sin(\omega_0t+\phi_0), \quad v_1=-r_0\omega_0\cos(\omega_0t+\phi_0),\\ x_2&=r_0\cos(\omega_0t+\phi_0), \quad v_2=r_0\omega_0\sin(\omega_0t+\phi_0). \end{aligned} \tag{14}$$

The frequency follows by estimations of the time the particle needs for one period moving on the circle with radius r_0 with constant speed v_0:

$$\omega_0=\frac{v_0}{r_0}=\left(\frac{a}{m}\right)^{1/2}=\omega. \tag{15}$$

This means, the particle oscillates even at strong pumping with the frequency given by the linear oscillator frequency ω (at least in our approximation).

The trajectory defined by the above four equations is like a hoop in the 4D space. Most projections to the 2D subspaces are circles or ellipses however there are two subspaces, namely, x_1-v_2 and x_2-v_1 where the projection is like a rod [20] .

Varying the initial conditions of the system a second limit cycle can be obtained. This limit cycle forms also a hula hoop that is different from the first one. However both limit cycles have the same projections on the $\{x_1,x_2\}$ and on the $\{v_1,v_2\}$ plane. The projection to the $\{x_1,x_2\}$ plane has the opposite sense of rotation in comparison with the first limit cycle. The separatrix between the two attractor regions is given by the following plane in the 4D space:

$$(\omega_0x_1-v_1)+(\omega_0x_2-v_2)=0. \tag{16}$$

Applying similar arguments to the stochastic problem we expect that the two hoops are converted into a distribution with the appearance of two embracing hoops with finite size, which for strong noise converts into two embracing hoops in the 4D phase space (see [20] for details). In order to obtain the explicit form of the distribution, we introduce the amplitude-phase representation

$$\begin{aligned} x_1&=\rho\sin(\omega_0t+\phi), \quad v_1=\rho\omega_0\cos(\omega_0t+\phi),\\ x_2&=\rho\cos(\omega_0t+\phi), \quad v_2=-\rho\omega_0\sin(\omega_0t+\phi), \end{aligned} \tag{17}$$

where radius ρ and phase ϕ are slow and fast stochastic variables, respectively. By using the standard procedure of averaging with respect to the fast phases we obtain for the Rayleigh model of pumping the following distribution of the radii:

$$P_0(\rho)\simeq\exp\left[\frac{\beta\omega_0^2}{D}\rho^2\left(\mu-\frac{1}{2}\omega_0^2\rho^2\right)\right]. \tag{18}$$

We see that the probability crater is surrounded by the two deterministic limit cycles (see Fig. 2). The full stationary probability in the 4D phase space has the form of two hula

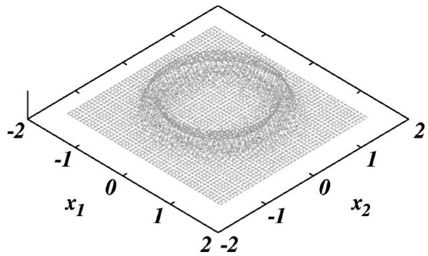

FIG. 2. Probability distribution $P_0(\rho)$ in the coordinate space $\{x_1,x_2\}$. One can easily see that the region of the most probable radii is located above the two limit cycles which were obtained from simulations. ($D=0.03$. All other parameters are set equal to 1.)

hoop distributions. The projections of the distribution onto the $\{x_1,x_2\}$ plane and to the $\{v_1,v_2\}$ plane are 2D rings. The hula hoop distribution intersects perpendicularly the $\{x_1,v_2\}$ plane and the $\{x_2,v_1\}$ plane. The projections to these planes are rodlike, and the intersection manifold with these planes consists of two ellipses located in the diagonals of the planes [20].

For an arbitrary initial condition one of two the rotational motions within the parabolic potential is excited. In the deterministic case this rotation remains a stable solution of the trajectory of one particle. To this rotation belongs a certain value of the angular momentum. For nonvanishing perturbations, e.g. white noise, the particle is able to cross the separatrix between the two rotational modes (limit cycles). In this case one can observe an inversion of the angular momentum of the particle [20].

IV. BIFURCATION ANALYSIS OF THE DYNAMICS OF A SYSTEM WITH AN ASYMMETRIC POTENTIAL

Without external fluctuations the system (1) has radial symmetry. In the mathematical context such dynamical systems are degenerate and structurally unstable. From the physical viewpoint, radial symmetry is a special situation, i.e., the gravitational field of point masses has strict radial symmetry and, therefore, this is true also for a two-dimensional mass-point pendulum. In real physical systems the radial symmetry is, in general, broken, e.g., a real pendulum in the earth field has no strict radial symmetry. Thus the oscillator with radial symmetry can only be considered as a particular case of corresponding real system that has some asymmetry. In addition to these general arguments we have some special motivation to study the case of broken radial symmetry. We plan the transition from external fields to mean fields generated by swarms of particles. First steps into this direction will be done in the last paragraph of this paper. However the mean field generated by a swarm will have no radial symmetry except the degenerate case that the swarm of particles and the forces have strict radial symmetry. In general swarms of particles can have a variety of rather complicated forms that leads to asymmetric mean fields. Thus our motivation is, to investigate the consequences of broken radial symmetry on the generation of rotational modes.

For the reasons explained above we will introduce into the model (1) a frequency mismatch between the partial subsystems. In this case the potential $U(r)$ has an elliptic, slightly extended shape. In other words, the expression for the symmetric potential Eq. (9) can be rewritten as follows:

$$U(x_1,x_2)=\frac{1}{2}(a_1x_1^2+a_2x_2^2), \tag{19a}$$

$$\sqrt{\frac{a_1}{a_2}}=\Delta=\frac{\omega_1}{\omega_2}. \tag{19b}$$

With this, the deterministic part of Eq. (1) leads to

$$\dot{x}_1=v_1, \quad \dot{v}_1=[\alpha-\beta(v_1^2+v_2^2)]v_1-\omega_1^2x_1, \tag{20a}$$

$$\dot{x}_2=v_2, \quad \dot{v}_2=[\alpha-\beta(v_1^2+v_2^2)]v_2-\omega_2^2x_2. \tag{20b}$$

For $\Delta\neq 1$ the system (20) is structurally stable or is one of the common propositions according to Arnold's nomenclature. It can describe the interaction of two oscillators, including the influence of noise.

To understand the dynamics of system (20), we first turn again to the symmetric case where $\omega_1^2=\omega_2^2$. We introduce a complex variable $z=x_1+jx_2$ by setting $\omega_1^2=\omega_2^2=\omega_0^2$. From Eq. (20) it follows that

$$\ddot{z}-\beta\left(\frac{\alpha}{\beta}-|\dot{z}|^2\right)\dot{z}+\omega_0^2z=0. \tag{21}$$

Equation (21) has periodic solutions of the form

$$z(t)=z\exp(\pm j\omega_0t)=|z|\exp(j\Phi)\exp(\pm j\omega_0t), \tag{22}$$

where the phase Φ takes any value in the interval $[0,2\pi]$. When we consider the symmetric case, we have an infinite number of periodic solutions [see Eq. (22)]. However, linear analysis cannot yield information about their stability. In numeric calculations, we can really detect six limit cycles (in the symmetric case). Each of them possesses its own type of symmetry. When there is a detuning ($\Delta\neq 1$), only two limit cycles remain stable, namely, Γ_1 and Γ_2 as described in detail in Sec. III. Further on we consider only these two.

Figure 3 shows projections of cycles Γ_1 and Γ_2 on different planes of the phase variables. It can be seen that the cycles are symmetric mirror images of one another. Therefore, we will perform the bifurcation analysis only for cycle Γ_1.

We estimate the stability of cycle Γ_1 by calculating its Floquet multipliers and registering the bifurcations when the multipliers reach the unit circle. A bifurcation diagram for the cycle Γ_1 on the $(\alpha-\Delta)$ plane is shown in Fig. 4 for fixed $\beta=1$ and $\omega_1=2$. Inside region I, we have the 1:1 resonance on a two-dimensional torus. The resonance domain is bounded by the bifurcation lines l_1 which correspond to a saddle-node bifurcation of cycle Γ_1 (its largest multiplier becomes equal to $+1$).

Cycle Γ_1 is stable inside the synchronization region I. When crossing the line l_1 the cycle merges with a relevant saddle cycle and disappears. The resonance structure on the

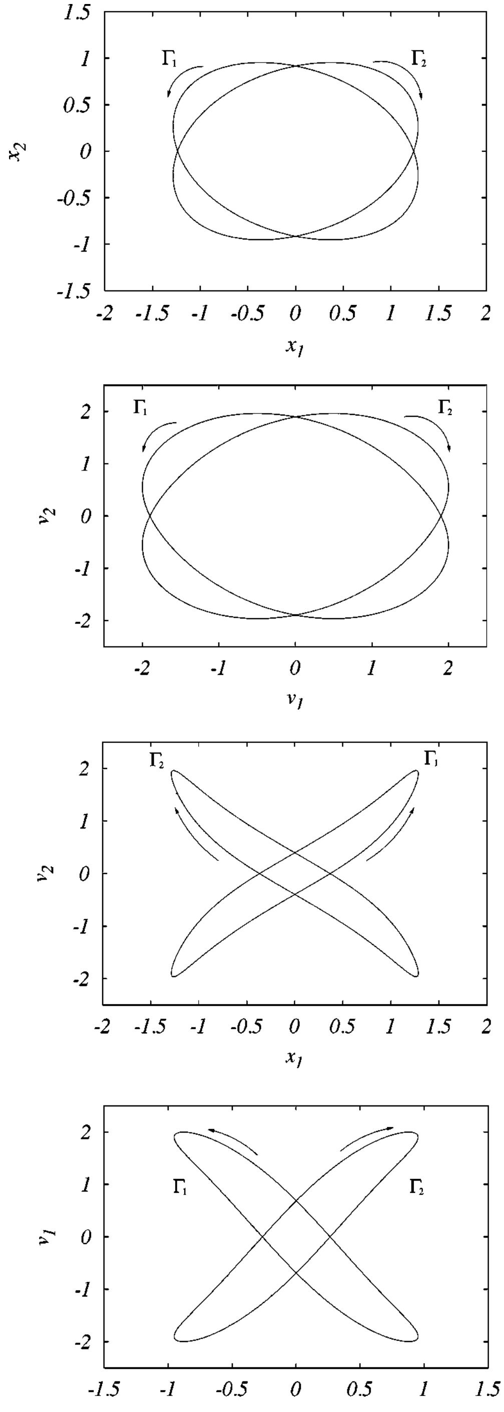

FIG. 3. Limit cycles of the detuned system without noise. The system kept two of six cycles found in the symmetric system. This is also an overview of the variety of cycles in the stabilization region I (see also Fig. 4).

torus is thus destroyed, and so the torus becomes ergodic. A full bifurcation diagram for system (20) is shown in Fig. 5 and illustrates a classical picture of Arnold's tongues corresponding to rational values of the winding number $\Theta = m:n,\ m,n = 1,2,\ldots$.

From a physical viewpoint, Fig. 5 testifies to the presence of multistability in the system (20). This phenomenon is conditioned by an overlapping of the resonance regions as the parameter α increases. This fact allows one to understand the peculiarities of the system response to external noise. For instance, inside the 1:1 region (region I in Fig. 4) the effect of noise causes the trajectory to wander in the neighborhoods of stable cycles Γ_1 and Γ_2 (see Fig. 6). Outside the synchronization region phase trajectories are more complicated and intertwined (see Fig. 7). Such behavior is determined by the presence of a large number of dynamical regimes in system (20), which include both ergodic and periodic trajectories.

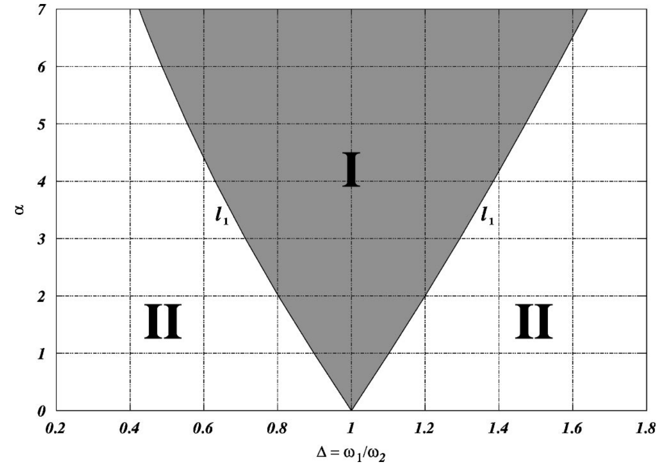

FIG. 4. Region of synchronization of the coupled oscillators for fixed $\beta = 1$ and $\omega_1 = 2$. Within the gray region (I) the limit cycles Γ_1 and Γ_2 are stable even under small perturbations (noise) (see also Fig. 7). The region represents the 1:1 resonance of a two-dimensional torus.

V. MOTION OF PAIRS, CLUSTERS, AND SWARMS

An application of the theoretical results given above, is the following: Let us imagine two Brownian particles that are pairwise bound to a dumb-bell-like configuration by a potential $U(|r_1 - r_2|)$ with parabolic shape. Then the motion consists of two independent parts: The free motion of the center of mass having the coordinates

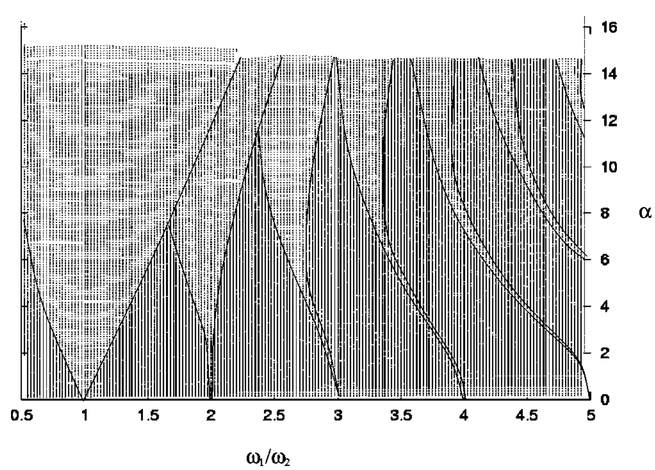

FIG. 5. Full bifurcation diagram of the system (20) showing the Arnold tongues.

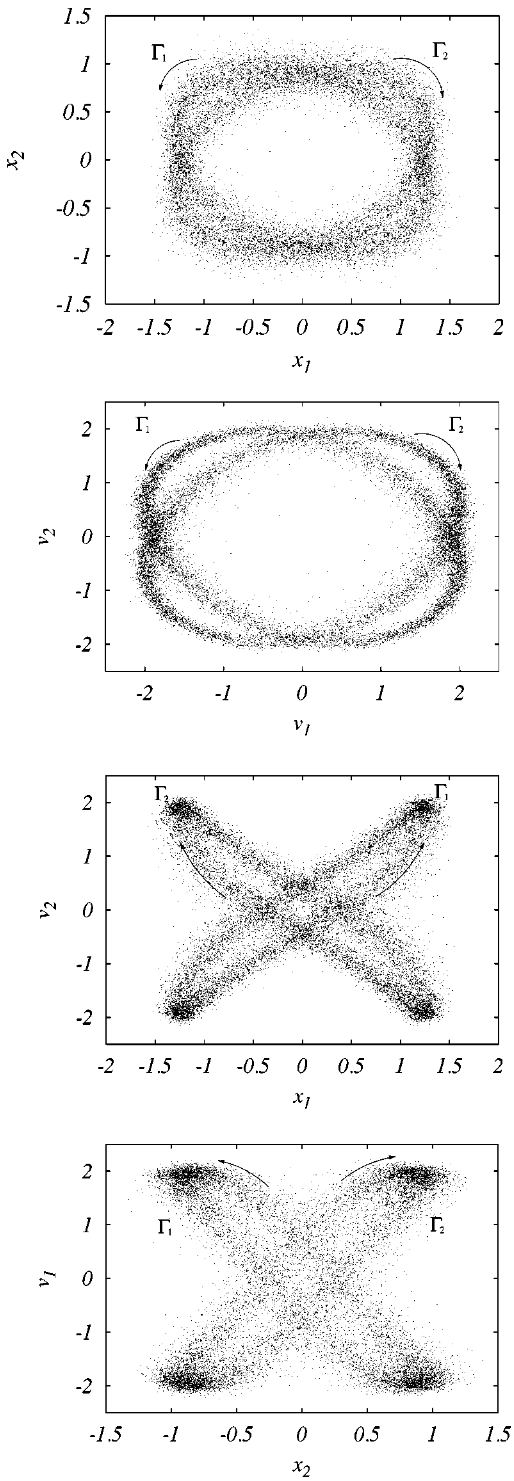

FIG. 6. Overview of the variety of cycles in the stabilization region I with noise. The stochastic trajectories are situated close to the deterministic cycles Γ_1 and Γ_2.

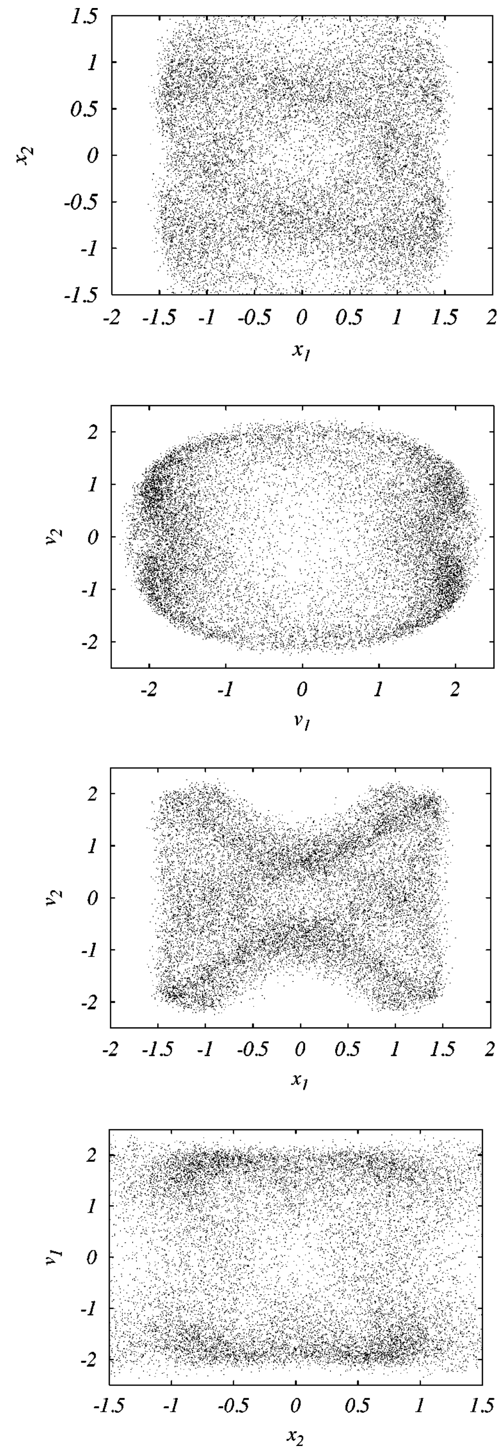

FIG. 7. Overview of the variety of cycles outside the stabilization region I with noise. The limit cycles are not stable anymore. The trajectories leave the 1:1 resonance and are situated on the full torus now.

$$X_1=\frac{1}{2}(x_{11}+x_{21});\quad X_2=\frac{1}{2}(x_{12}+x_{22}), \tag{23}$$

and the relative motion described by the coordinates

$$\tilde{x}_1=x_{11}-x_{12};\quad \tilde{x}_2=x_{12}-x_{22}, \tag{24}$$

under the influence of the potential. The motion of the center of mass M is approximately described by the equations:

$$\dot{X}_1=V_1,\quad M\dot{V}_1=-\gamma(V_1,V_2)V_1,$$
$$\dot{X}_2=V_2,\quad M\dot{V}_2=-\gamma(V_1,V_2)V_2. \tag{25}$$

Further the relative motion is approximately described by the equations:

$$\dot{\tilde{x}}_1 = \tilde{v}_1, \quad \frac{1}{2}\dot{\tilde{v}}_1 = -\gamma(\tilde{v}_1, \tilde{v}_2)\tilde{v}_1 - a_1 \tilde{x}_1, \tag{26a}$$

$$\dot{\tilde{x}}_2 = \tilde{v}_2, \quad \frac{1}{2}\dot{\tilde{v}}_2 = -\gamma(\tilde{v}_1, \tilde{v}_2)\tilde{v}_2 - a_1 \tilde{x}_2. \tag{26b}$$

As a consequence, the center of mass of the dumb bell will make a driven Brownian motion, but in addition the dumb bell is driven to rotate around its center of mass. What we observe then is a system of pumped Brownian molecules which, with respect to their center of mass velocities, have a distribution corresponding to Eq. (8). However the internal degrees of freedom are also excited and we observe driven rotations and, in general, oscillations also. In this way we have shown that the mechanisms described here may be used also to excite the internal degrees of freedom of Brownian molecules.

An extension of this theory of pairs can be an application to the motion of clusters of active particles. Let us assume that the interaction of the particles within the cluster is given by a van der Waals shaped interaction with a relatively long range tail. For example, we may use the interaction model proposed by Morse [31,32]

$$\phi_{ij} = \frac{A}{2b}[(e^{-b(r-\sigma)} - 1)^2 - 1]. \tag{27}$$

Because of the attracting tail the particles will bind to the clusters. The individual particles then move in the collective field of the other particles. This can be represented in a mean field approximation,

$$V(\tilde{\boldsymbol{r}}) = \int d\boldsymbol{r}'\, \phi(\tilde{\boldsymbol{r}} - \boldsymbol{r}')\rho(\boldsymbol{r}'), \tag{28}$$

where $\tilde{\boldsymbol{r}} = (\tilde{x}_1, \tilde{x}_2)$ is the radius vector counted from the center of mass, and $\rho(\boldsymbol{r}')$ is the mean density within the cluster. Approximating V by a quadratic,

$$V(\tilde{x}_1, \tilde{x}_2) = V_0 + \frac{1}{2}(a_1 \tilde{x}_1^2 + a_2 \tilde{x}_2^2) + \cdots, \tag{29}$$

we arrive again at the harmonic problem we have studied above. In general, due to the asymmetries of the shape of a the swarm we will have $a_1 \neq a_2$. In other words, the individual particles in the cluster move, at least in a certain approximation, in an asymmetric parabolic potential. This is responsible for the excitation of an angular momentum. As a result of this we observe rotating clusters of Brownian particles that change the direction of rotation due to the influence of noise (see Figs. 8 and 9). Due to the noise induced perturbations the excited angular momentum changes sign randomly as well (Fig. 9).

The aforementioned model application may be interesting, for example, to biologists, since it describes vortex-type motions that change direction spontaneously and randomly

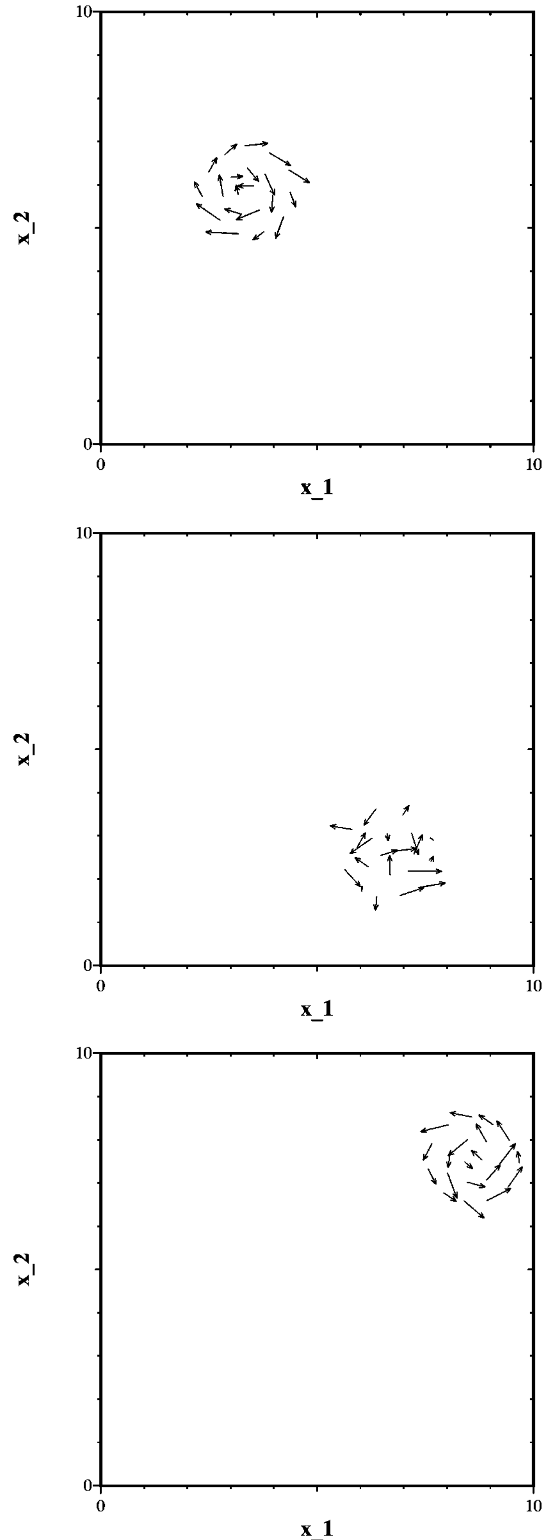

FIG. 8. Rotating cluster of 20 particles for different time steps. The arrows correspond to the velocity of the single particle. Because of the influence of noise the cluster changes the direction of rotation randomly.

as observed under certain conditions with actual biological swarms [33] . Similarly to the case of the dumb bells, the clusters will be driven to make spontaneous changes in the directions of rotation. Finally a stationary state will be

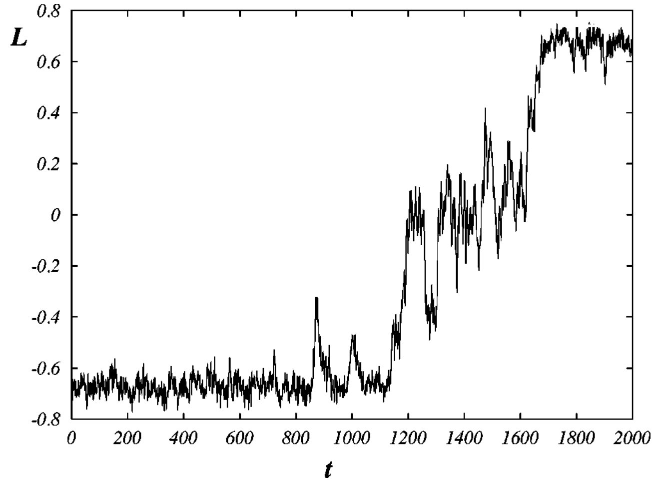

FIG. 9. Evolution of the angular momentum of the cluster. One can see that it stochastically changes the sign.

reached that is a mixture of rotating clusters. With increasing asymmetry of the shape of the cluster or swarm, the differences between a_1 and a_2 will increase. Consequently we can predict, according to our findings in Sec. IV, that strongly nonsymmetric clusters, will switch from more or less regular rotations to more irregular motions. The overlapping structure of the Arnold tongues in Fig. 5 suggests that the irregular motion can be chaotic.

VI. DISCUSSION

The main objective of this work was to study the influence of linear attracting forces on active Brownian particles. We studied both external forces and particle-particle interaction forces as well.

The basic assumption was to add to the dynamics of simple physical Brownian particles a different mechanism: pumping with free energy. This was realized by including energy uptake into a depot, and simultaneous conversion of the energy into mechanical motion, with stochastic influences. In this way, as we have shown, motions of the particles become more complex, showing different dynamical features and, in particular, the appearance of rotational modes. The main topic of this investigation was the study of linear forces that do not possess the property of radial symmetry acting on the particles. We have shown that with increasing asymmetry the limit cycles describing the rotational modes are destroyed, and the bifurcation diagram shows typical Arnold tongues. This might affect the behavior of clusters or swarms that typically perform left or right rotations but may switch to an irregular dynamics if the asymmetry is large enough.

From summarizing the results above one can deduce that the combination of self-propelling features with particle-particle interaction forces that form a mean field to every particle can resemble vortex-type motions. The connection of the nonlinear driving forces with paraboliclike mean fields shows stable rotational modes within the first Arnold tongue. The higher the energy uptake rate the more asymmetric the mean field can be for stable rotations of the clusters. If the rotational modes are destroyed it is due to the increasing asymmetry of the cluster or due to the decreasing energy uptake of the single particles.

Therefore the shown model may resemble active biological motion. At least it could be a first ansatz to model biological systems that show swarming behavior with vortex-type modes. The advantage of the model is the simplicity of the system of equations. It would be very easy to apply this approach to more concrete biological systems. In order to avoid misunderstandings we underline, that we did not intend here to model any particular nonphysical object. Instead we analyze particular physical, nonequilibrium systems that show new types of dynamics. These results might be of interest for later, more concrete applications in particular to the dynamics of swarms.

ACKNOWLEDGMENTS

The authors acknowledge fruitful discussions with F. Moss (University of Missouri, St. Louis) and L. Schimansky-Geier (Humboldt-University, Berlin, Germany). Furthermore, assistance by J. Dunkel (Humboldt-University, Berlin, Germany) with some numerics is acknowledged. This work was partly supported by the Humboldt Foundation (V.S.A.) and the Sfb 555 ''Complex Nonlinear Processes'' of the German Science Foundation (DFG) (W.E. and U.E.)

[1] T. Vicsek, A. Czirók, E. Ben-Jacob, I. Cohen, and O. Shochet, Phys. Rev. Lett. **75**, 1226 (1995).
[2] J. Toner and Y. Tu, Phys. Rev. Lett. **75**, 4326 (1995).
[3] C.-H. Chiang and L. I, Phys. Rev. Lett. **77**, 647 (1996).
[4] A. Czirók, E. Ben-Jacob, I. Cohen, and T. Vicsek, Phys. Rev. E **54**, 1791 (1996).
[5] A. Czirók, H.E. Stanley, and T. Vicsek, J. Phys. A **30**, 1375 (1997).
[6] E. Ben-Jacob, I. Cohen, A. Czirók, T. Vicsek, and D. Gutnick, Physica A **238**, 181 (1997).
[7] J. Toner and Y. Tu, Phys. Rev. E **58**, 4828 (1998).
[8] A. Czirók, A.-L. Barabási, and T. Vicsek, Phys. Rev. Lett. **82**, 209 (1999).
[9] W.-J. Rappel, N. Alastair, S. Armand, and H. Levine, Phys. Rev. Lett. **83**, 1247 (1999).
[10] A.S. Mikhailov and D. Zanette, Phys. Rev. E **60**, 4571 (1999).
[11] D. Helbing, I.J. Farkas, and T. Vicsek, Phys. Rev. Lett. **84**, 1240 (2000).
[12] D. Helbing, I.J. Farkas, and T. Vicsek, Nature (London) **407**, 487 (2000).
[13] H. Levine, W.-J. Rappel, and I. Cohen, Phys. Rev. E **63**, 017101 (2001).
[14] A. Czirók, M. Matsushita, and T. Vicsek, Phys. Rev. E **63**, 031915 (2001).
[15] X.H. Zheng and J.C. Earnshaw, Phys. Rev. Lett. **75**, 4214 (1995).

[16] Z. Csahók and T. Vicsek, Phys. Rev. E **52**, 5297 (1995).
[17] D. Helbing, F. Schweitzer, J. Keltsch, and P. Molnár, Phys. Rev. E **56**, 2527 (1997).
[18] W. Ebeling, F. Schweitzer, and B. Tilch, BioSystems **49**, 17 (1999).
[19] F. Schweitzer, W. Ebeling, and B. Tilch, Phys. Rev. Lett. **80**, 5044 (1998).
[20] U. Erdmann, W. Ebeling, F. Schweitzer, and L. Schimansky-Geier, Eur. Phys. J. B **15**, 105 (2000).
[21] Y.L. Klimontovich, Usp. Fiz. Nauk **164**, 811 (1994) [Phys. Usp. **37**, 737 (1994)].
[22] M. Schienbein and H. Gruler, Bull. Math. Biol. **55**, 585 (1993).
[23] I. Derényi and T. Vicsek, Phys. Rev. Lett. **75**, 374 (1995).
[24] M. Bier and R.D. Astumian, Phys. Rev. Lett. **76**, 4277 (1996).
[25] A. Czirók and T. Vicsek, Physica A **281**, 17 (2000).
[26] O. Steuernagel, W. Ebeling, and V. Calenbuhr, Chaos, Solitons Fractals **4**, 1917 (1994).
[27] J.W. Rayleigh, *The Theory of Sound*, 2nd ed. (Dover, New York, 1945), Vol. I.
[28] W. Ebeling, U. Erdmann, L. Schimansky-Geier, and F. Schweitzer, in *Stochastic and Chaotic Dynamics in the Lakes*, edited by D.S. Broomhead, E.A. Luchinskaya, P.V.E. McClintock, and T. Mulin, AIP Conf. Proc. No. 502 (AIP, Melville, NY, 2000), pp. 183–190.
[29] L. Fronzoni, R. Manella, P.M.V. McClintock, and F. Moss, Phys. Rev. A **36**, 834 (1987).
[30] L. Fronzoni, F. Moss, and P.M.V. McClintock, Phys. Rev. A **36**, 1492 (1987).
[31] P.M. Morse and E.C.G. Stueckelberg, Phys. Rev. **33**, 932 (1929).
[32] P.M. Morse, Phys. Rev. **34**, 57 (1929).
[33] F. Moss (private communication).